Journal of Sea Research 133 (2018) 2–10

Contents lists available at ScienceDirect

Journal of Sea Research

journal homepage: www.elsevier.com/locate/seares

# Examination of a high resolution laser optical plankton counter and FlowCAM for measuring plankton concentration and size

Jocelyn Kydd [a,*], Harshana Rajakaruna [a], Elizabeta Briski [b], Sarah Bailey [a]

[a] Great Lakes Laboratory for Fisheries and Aquatic Sciences, Fisheries and Oceans Canada, 867 Lakeshore Road, Burlington, ON L7R 4A6, Canada
[b] GEOMAR Helmholtz Centre for Ocean Research, Düsternbrooker Weg 20, 24105 Kiel, Germany

ARTICLE INFO

*Article history:*
Received 12 September 2016
Received in revised form 21 December 2016
Accepted 18 January 2017
Available online 19 January 2017

*Keywords:*
Ballast water
Compliance monitoring
Indicative analysis
Particle abundance
Particle size
Size frequency distribution

ABSTRACT

Many commercial ships will soon begin to use treatment systems to manage their ballast water and reduce the global transfer of harmful aquatic organisms and pathogens in accordance with upcoming International Maritime Organization regulations. As a result, rapid and accurate automated methods will be needed to monitoring compliance of ships' ballast water. We examined two automated particle counters for monitoring organisms ≥50 μm in minimum dimension: a High Resolution Laser Optical Plankton Counter (HR-LOPC), and a Flow Cytometer with digital imaging Microscope (FlowCAM), in comparison to traditional (manual) microscopy considering plankton concentration, size frequency distributions and particle size measurements. The automated tools tended to underestimate particle concentration compared to standard microscopy, but gave similar results in terms of relative abundance of individual taxa. For most taxa, particle size measurements generated by FlowCAM ABD (Area Based Diameter) were more similar to microscope measurements than were those by FlowCAM ESD (Equivalent Spherical Diameter), though there was a mismatch in size estimates for some organisms between the FlowCAM ABD and microscope due to orientation and complex morphology. When a single problematic taxon is very abundant, the resulting size frequency distribution curves can become skewed, as was observed with *Asterionella* in this study. In particular, special consideration is needed when utilizing automated tools to analyse samples containing colonial species. Re-analysis of the size frequency distributions with the removal of *Asterionella* from FlowCAM and microscope data resulted in more similar curves across methods with FlowCAM ABD having the best fit compared to the microscope, although microscope concentration estimates were still significantly higher than estimates from the other methods. The results of our study indicate that both automated tools can generate frequency distributions of particles that might be particularly useful if correction factors can be developed for known differences in well-studied aquatic ecosystems.



## 1. Introduction

Ballast water is a well-known vector for introducing nonindigenous species that have caused negative economic and ecological effects around the world (Carlton, 1985; Carlton and Geller, 1993; Ruiz et al., 2000; Bailey, 2015). To reduce the threat of harmful aquatic organisms and pathogens, the International Maritime Organization (IMO) adopted the International Convention for the Control and Management of Ships' Ballast Water and Sediments in 2004. After entry into force, ships will be required to meet the discharge standards set out in Regulation D-2, which specifies that discharged ballast water shall contain <10 viable organisms ≥50 μm in minimum dimension per cubic meter; <10 organisms between ≥10 and <50 μm in minimum dimension per milliliter; and additional limits for indicator bacteria (IMO, 2004). Most ships are expected to meet this regulation by installing ballast water treatment systems; rapid and accurate methods to enumerate and measure microscopic organisms will be needed to confirm that treated ballast water meets the discharge standards and that the risk of introduction of species into the environment has been reduced.

There have been promising advances in automating assessments of organisms <50 μm in minimum dimension using tools such as PAM fluorometry and flow cytometry (Veldhuis and Fuhr, 2008; Bradie, 2016), but little progress has been made for organisms ≥50 μm (First and Drake, 2012; Zetsche and Meysman, 2012). Organisms in the ≥50 μm size range are typically zooplankton, but can include larger phytoplankton as well. Currently, the standard procedure for enumerating viable organisms ≥50 μm involves expert assessment under a suitable microscope (Jørgensen et al., 2010). Depending on the volume needed to measure for compliance and the concentration of particles (live/dead organisms and debris) in the sample, this procedure can be time consuming, taking up to six hours for a well-trained analyst to count

* Corresponding author.
*E-mail addresses:* Jocelyn.Kydd@dfo-mpo.gc.ca (J. Kydd), Harshana.Rajakaruna@dfo-mpo.gc.ca (H. Rajakaruna), ebriski@geomar.de (E. Briski), Sarah.Bailey@dfo-mpo.gc.ca (S. Bailey).

http://dx.doi.org/10.1016/j.seares.2017.01.003

viable organisms in ~75 mL water volume (First and Drake, 2012). Speeding up this process with a reliable, automated method would reduce organism mortality caused by deteriorating environmental conditions during sample holding and processing, reduce errors related to fatigue of the analyst and reduce the time required for ballast water compliance testing. Here, we examined two potential automated methods for counting organisms ≥50 μm: a High Resolution Laser Optical Plankton Counter (HR-LOPC) and a Flow Cytometer with digital imaging Microscope (FlowCAM®).

Laser Optical Plankton Counters have been used to rapidly determine the size distribution and abundance of zooplankton in natural aquatic systems (Finlay et al., 2007a; Finlay et al., 2007b; Schultes and Lopes, 2009; Gaardsted et al., 2011; Rahkola-Sorsa et al., 2014). In the laboratory, a sample circulator component can be added to assess samples (live or preserved) (Finlay et al., 2007a; Gaardsted et al., 2010; Rahkola-Sorsa et al., 2014; Mines et al., 2013). The standard LOPC counts and measures particles >100 μm as they pass a laser beam (Herman et al., 2004); we examined the potential of a High Resolution LOPC modified to enumerate particles between 20 μm to 12 mm (Rolls Royce Canada Ltd. – Naval Marine). Though the HR-LOPC cannot determine particle status (live organism, dead organism or detritus), it has the ability to analyse a large volume sample in minutes.

The FlowCAM (Fluid Imaging Technologies, Inc.) has been used mainly for analyzing particles <200 μm (Sieracki et al., 1998; Álvarez et al., 2011, 2012, 2014) with one publication to date for zooplankton (Le Bourg et al., 2015). The FlowCAM combines flow cytometry, microscopy and image analysis to automate the enumeration and measurement of particles from 3 to 3000 μm (Sieracki et al., 1998). Images captured by the FlowCAM can be used to discriminate plankton from detritus manually or by using automated classification software (Zarauz et al., 2009; Álvarez et al., 2012, 2014). It also has the ability to detect fluorescence for assessing viability (Steinberg et al., 2012), though this was not investigated here. The FlowCAM can rapidly image numerous particles but sample analysis can be time consuming when particle concentrations or sample volumes are high (Álvarez et al., 2011).

As a first step to assess the potential of the HR-LOPC and the FlowCAM as potential tools for indicative analysis of organisms ≥50 μm in ballast water, this study examines the accuracy of automated particle counts, size frequency distributions and particle size measurements in comparison to data generated by traditional light microscopy as a baseline. In addition, we conducted finer scale comparisons of the FlowCAM and the microscope to evaluate measurements according to taxonomic group.

## 2. Methods

### 2.1. Sample preparation

One plankton sample was collected from Hamilton Harbour, Lake Ontario, in December 2012 by combining 15 vertical net hauls (4 m to surface) using a 30 cm diameter conical plankton net with 30 μm (~50 μm in diagonal) mesh. The sample was condensed into a 1 L bottle and preserved in 70% ethanol. A Folsom splitter was subsequently used to split half the sample into 16 equal fractions, each equal to 132.5 L of original harbour water. These fractions were used as replicate samples by randomly assigning five sample fractions (replicates) to each of the three measurement treatments: HR-LOPC, FlowCAM and microscope. The replicate samples were kept in 70% ethanol until analysis (preparation steps summarized in Fig. 1). The samples were removed from the ethanol using a 20 μm Nitex mesh sieve and placed in distilled water prior to analysis for all treatments.

### 2.2. HR-LOPC

A sample circulator was used with the HR-LOPC to obtain counts and size measurements of particles in each replicate. Each replicate sample was suspended in 50 mL of distilled water, poured slowly into the sampling chamber below the surface of the water using a funnel with attached tube to prevent air bubbles from entering the system and run through the circulator for 20 min. The detection threshold was set at 77, limiting the HR-LOPC to capture particles >30 μm, as recommended by Rolls Royce Canada, Ltd. The particle data was examined using a modified post processing program (LOPC PostPro, Rolls Royce Canada Ltd. – Naval Marine) to produce a distribution plot of particle sizes in 15-μm bins.

### 2.3. FlowCAM®

The broad size range of plankton being analysed (30 to 1000 μm) was examined using multiple field-of-view (FOV) flow cells (80, 300 and 1000 FOV) and corresponding microscope objectives (100, 40 and 10×). Particles contained in each replicate were separated according to flow cell size using a series of Nitex mesh sieves (75, 295, and 1000 μm), with each fraction rinsed into a 50 mL bottle with 70% ethanol until analysis. Prior to analysis, each fraction was initially put into a measured volume of distilled water. For the two larger sized fractions, a subsample of this initial volume was diluted into a solution of polyvinylpyrrolidone (PVP), M.W. 1,300,000 to increase the viscosity of the liquid, slowing the descent of the larger particles through the flow cell to improve capture rates by the digital camera (as recommended by the manufacturer and verified by preliminary experiments).

The <75 μm fractions were suspended in 40 mL distilled water. Using an Eppendorf pipette, a 3 mL aliquot was processed using the 80 μm, 5 mm FOV flow cell with the 10× objective (100× magnification). The particle-dense <75 μm fractions were analysed using AutoImage mode, where images are captured at set intervals. The volume of sample analysed was calculated by the software based on the number of images taken, the field of view, and the depth of the flow cell. The sample was added in 0.5 mL increments to prevent settling of particles. At 33% efficiency (calculated based on the image capture rate in the Autoimage mode and the flow of sample), 1 mL of the 3 mL aliquot was counted in 60 min. The 75–295 μm fractions were suspended in 20 mL of distilled water. From the 20 mL, 2.5 mL was diluted to 10–15 mL in a 2.5% solution of PVP to get one particle per image and then processed using the 300 μm, 5 mm FOV flow cell with the 4× objective (40× magnification). Scatter Trigger mode was used, with images taken only when the laser light (532 nm) was disrupted by a passing particle, rather than at set intervals as in AutoImage mode. The volume of the sample analysed was calculated by the software based on the field of view, depth of the flow cell and the total volume of fluid that passed through the flow cell. For the 75–295 μm fraction, sampling time varied from 20 to 30 min depending on the volume processed. For the 295–1000 μm fractions, the sample was initially put into 40 mL of distilled water; 20 mL was removed and diluted in 2.5% PVP to a volume of 60 mL for rep 1 and 80 mL for reps 2 to 4. These were processed with a 1000 FOV flow cell and 2× objective (20× magnification) using Scatter trigger mode. For the 295–1000 μm fraction, sampling time varied from 30 to 45 min depending on the volume processed.

Particle counts and measurement data were determined using Fluid Imaging's VisualSpreadsheet© (VSS) software. Data from the three size fractions were subsequently pooled into a composite count for each sample. The captured images allowed for visual classification into taxonomic groups with the aid of sorting and filtering features in the VSS program for concentration and size comparisons against the microscope data, by taxonomic group. One of the five replicate samples for the FlowCAM was poorly preserved as evident from the number of decaying organisms imaged and was excluded from further analysis.

### 2.4. Microscope

Zooplankton and phytoplankton were enumerated separately on an AZ100 Nikon multipurpose microscope at 10× to 400× magnification,

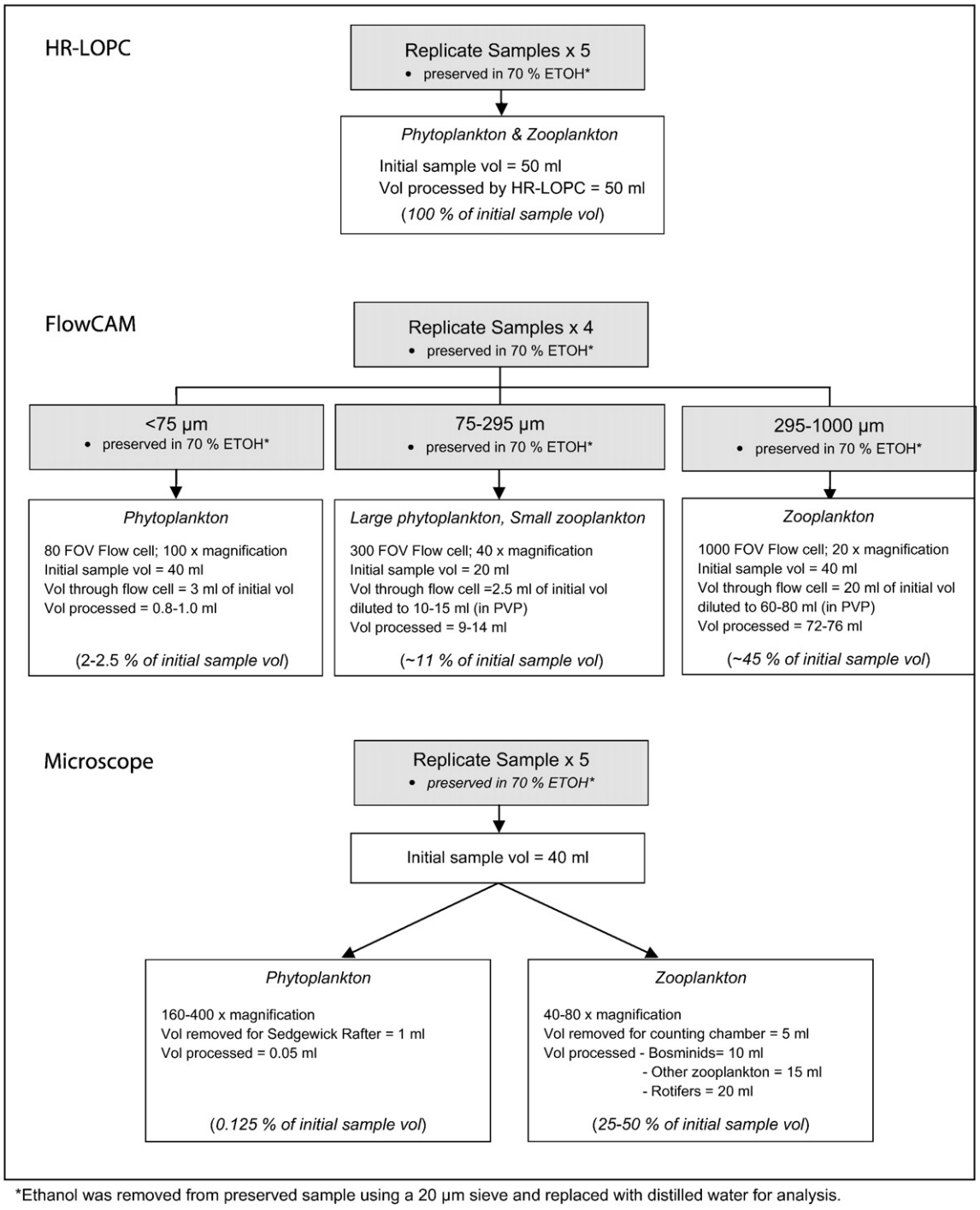


**Fig. 1.** Flow chart for samples processed on the HR-LOPC, FlowCAM, and microscope including details of volumes (vol) used and magnification. Initial sample vol = the concentrated sample volume in distilled water after ethanol was removed; FOV = Field of View; PVP = 2.5% polyvinylpyrrolidone solution.

equipped with a QImaging Retiga 2000R camera and AIS Element imaging software. Zooplankton were analysed by suspending each replicate in 40 mL of distilled water. Subsamples were removed with a 5 mL Henson-Stempel pipette for analysis. Multiple subsamples were analysed until at least 200–300 individuals were counted (a maximum of 100 organisms for any one taxon), or until 50% of the sample was analysed. Individuals were classified into taxonomic groups, typically at the level of Order or Genus. Length and width of 30 individuals per crustacean taxon and 20 individuals per rotifer taxon were measured under 40–80× magnification. Caudal rami and spines were excluded from length measurements, and width was measured as the widest part of the body perpendicular to the length. With measurements, each sample took 3–4 h to complete analysis.

Phytoplankton were analysed by suspending each replicate in 40 mL of distilled water. Subsamples (1.1 mL) were removed with a pipette for analysis using a Sedgewick Rafter counting chamber under 160–400× magnification. The sample was allowed to settle for 30 min prior to assessment. 200–250 phytoplankton particles were counted to determine density. Length and width were measured for 30 plankton particles per taxonomic group. To parallel measurements generated by HR-LOPC and FlowCAM, phytoplankton colonies were measured as one particle, though for the first ten colonies of each taxon 3 individual cells were

also measured. For the phytoplankton, processing counts and measurements took approximately 3 h.

### 2.5. Particle measurements

Standard calibration beads were used to verify size measurements according to manufacturer recommendations for the FlowCAM and HR-LOPC, and a micrometer was used to calibrate microscope software, prior to use.

Equivalent spherical diameter (ESD), typically defined as the diameter of a sphere having equivalent volume as the particle of interest, was estimated by each instrument using slightly different methods. The LOPC ESD is calculated based on the occultation of the laser beam, as captured by an array of 35 photodiode elements (Herman et al., 2004). To allow for capturing particles between 20 μm to 12 mm, the HR-LOPC was modified to have 0.3 × 0.3 mm elements in the photodiode array versus the 1 × 1 mm elements in the standard LOPC (Rolls Royce Canada Ltd. – Naval Marine). The HR-LOPC ESD was generated for every particle in the sample as the diameter of a circle having equivalent area to the estimated area of the particle of interest.

The FlowCAM can generate two ESD measurements. The first, referred to as the FlowCAM ESD, is calculated based on the mean of 36 feret measurements taken around the particle. The second, Area Based Diameter (FlowCAM ABD), is based on the area of pixels that make up the image of the particle calculated to the diameter of a circle with an equivalent area. Both ESD measurements are calculated for every particle processed by the FlowCAM. Additionally, the FlowCAM provides length and width measurements for every particle that can be used to manually calculate ESD in the same manner as is typical for traditional microscope measurements (see next).

On the microscope, ESD was calculated using the geometric mean of the measurements: $(\text{length} \times \text{width})^{0.5}$ (Beaulieu et al., 1999). Additionally, a cell area-based ESD ($ESD_A$) was calculated for *Asterionella*, a colonial species made up of long, thin cells set in a star shape with a lot of interstitial space between the cells (Fig. 2A). To calculate $ESD_A$, the length and width of three individual cells per colony were measured; the average length and average width of the three cells was multiplied to calculate an average area per cell and multiplied by the number of cells in that colony to estimate the area of the colony ($A$). The $ESD_A$ was then calculated using the equation $ESD_A = 2(A/\pi)^{0.5}$. The $ESD_A$ was calculated for 10 colonies per replicate.

### 2.6. Particle classification

Particles on the FlowCAM and microscope were classified into major taxonomic groups. Zooplankton included Calanoida, Cyclopoida, copepod naupli, Bosminids, *Daphnia*, *Asplanchna*, *Keratella*, *Polyarthra*, and *Kellicottia*. Phytoplankon were grouped as *Asterionella*, *Fragilaria*, *Stephanodiscus*, *Closteriopsis*, *Oscillatoria*, *Codonella*, *Microcystis*, *Cryptophyceae*, *Staurastrum*, *Pediastrum*, and *Tabellaria*. Rare taxa or unidentified organisms were categorized as 'other' rotifers, zooplankton, or phytoplankton. Non-organism particles imaged by the FlowCAM were classified as debris; duplicate images, images of bubbles, or of the flow cell itself were manually deleted.

### 2.7. Data analysis

All concentration data were standardized to a 1 L volume to account for variation in volumes analysed across replicates. FlowCAM and microscope data were grouped into 15 μm bins to match the HR-LOPC output. As the distribution of particles in the 15 μm bins declined exponentially from initial to later bins, the data was further standardized by grouping the bins using an octave scale (base 2), i.e. >30–60 μm, >60–135 μm…>1020 μm (Beaulieu et al., 1999). As the detection threshold of the HR-LOPC was limited to particles >30 μm, particles <30 μm captured by FlowCAM or microscope were omitted from comparisons with the HR-LOPC; the smaller particles were used only for comparisons of FlowCAM and microscope. Comparisons of FlowCAM and HR-LOPC considered total particle data, including both organisms and debris since the HR-LOPC does not differentiate particles. Debris was removed from FlowCAM data for comparisons with microscope data. We conducted comparisons of size measurements across devices, considering the automated ESD outputs from the instruments (HR-LOPC ESD, FlowCAM ESD and FlowCAM ABD) against manual calculations of ESD by microscope. Manual calculations of ESD based on particle length and width from the FlowCAM, completed in the same manner as for the microscope, were not significantly different from the automated FlowCAM ESD output; thus, only comparisons based on the automated outputs of the devices are presented in this paper.

The density of particles counted per sample by each device was compared using one-way analysis of variance (ANOVA), except for comparisons of FlowCAM ABD versus FlowCAM ESD, where a paired-sample *t*-test was used (SYSTAT 13) because the measurements originated from the same replicates. A *Hotelling T-squared* test for two multivariate

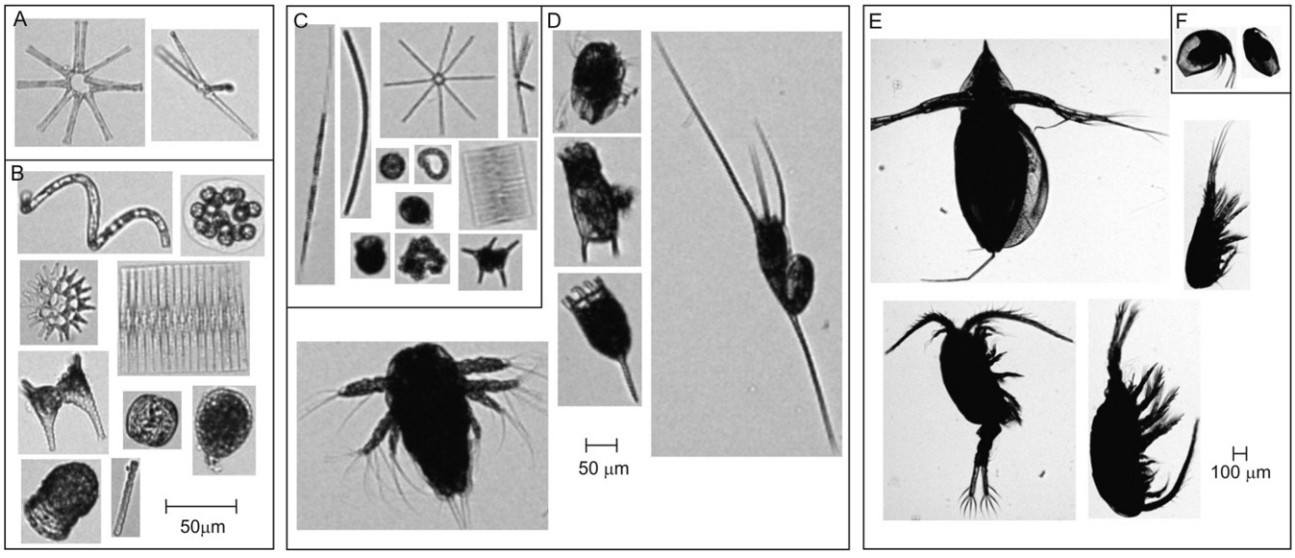


**Fig. 2.** Examples of (A,B,C) phytoplankton and (D,E,F) zooplankton taxa captured digitally by the FlowCAM divided into three size groups: (A, B) 20–75 um, (C,D) 75–295 um, and (E, F) 295–1000 um. (A) *Asterionella* and (F) *Bosmina* are shown in two orientations.

independent samples (with equal and unequal covariance matrices, as appropriate) was used to test for differences in concentration estimates at different size classes (MATLAB). Three size classes were used for this analysis: > 30–60 μm, >60–135 μm, and >135 μm. The size classes > 135 μm were grouped as one because the concentration of particles > 255 μm was negligibly small compared to other categories. Also, using more than three size classes would violate the assumptions of the test, since the smallest number of replicates for any method was four. The relative frequencies of densities by size classes were also tested using the two sample Kolmogorov-Smirnov (K-S) test with a Markov chain Monte Carlo method, comparing two methods at a time for significance in frequency distributions using the null $H_o$: Both methods capture the same size frequency in the population.

Additional comparisons were conducted between FlowCAM and microscope to evaluate measurements according to taxonomic group. This analysis was limited to taxonomic groups with >15 individuals. Comparisons were conducted using ANOVA with Bonferroni correction (SYSTAT 11). To increase the sample size, the mean organism ESD was based on all particles measured by the instrument irrespective of the individual replicates, since all the particles originated from the same net haul sample (i.e., the same population).

## 3. Results

Estimates of sample particle concentration were highly variable across devices, with the highest counts recorded by microscope (1348.40 ± 171.07 organisms > 30 μm $L^{-1}$), and the lowest by HR-LOPC (91.97 ± 7.25 particles > 30 μm $L^{-1}$) (Table 1). Concentration estimates were significantly different, both considering the total number of particles per sample (one-way ANOVA, $F = 89.91$, $df = 3, 14$, $p < 0.001$), and when examining densities given the variation also among the size classes (Fig. 3A, Table 2). After concentration estimates were converted to relative frequencies, microscope and FlowCAM ESD (*Kolmogorov-Smirnov*, $p = 0.54$), and FlowCAM ABD and HR-LOPC (*Kolmogorov-Smirnov*, $p = 0.53$) measures were not statistically different, while remaining paired comparisons between methods were significantly different (Fig. 3B, Table 2).

For the more abundant phytoplankton and zooplankton taxonomic groups, concentration estimates were approximately 60% lower on the FlowCAM compared to the microscope (Fig. 4). The FlowCAM captured a large number of particles allowing assessment of more taxonomic groups (34 taxa) compared to the microscope (27 taxa). Both instruments gave similar results in terms of relative abundance of individual taxa, with *Asterionella* sp. being the most abundant taxon comprising 58.6 ± 4.1% of the sample on the FlowCAM and 56.5 ± 4.4% on the microscope, followed by *Fragilaria*, *Microcystis* and *Pediastrium*. The sample contained mostly colonial species, with few non-colonial cells <50 μm and few organisms measuring >50 μm. Fig. 2 shows examples of some of the organisms imaged by the FlowCAM.

Fig. 5 shows the size comparison of different taxa measured on FlowCAM, using both ESD and ABD, and on the microscope. The FlowCAM ABD measurements were similar to microscope ESD measurements, except for *Asterionella sp.*, *Staurastrum* sp. and *Closteriopsis sp.* (ANOVA with Bonferroni, $p < 0.0001$). The FlowCAM ESD generally produced larger size estimates relative to the FlowCAM ABD and the microscope ESD. In all cases the FlowCAM ESD was significantly different from the FlowCAM ABD and in most cases significantly different from the microscope (ANOVA with Bonferroni, $p < 0.0001$). Of all the taxa compared, *Asterionella* was an unusual case where the FlowCAM ABD (41.6 ± 15.7 μm; $n = 10.022$) underestimated the size by 58% compared to the microscope ESD (98.2 ± 29.3 μm, $n = 150$). The FlowCAM ESD (98.5 ± 31.5, $n = 10.022$) was the same as the microscope ESD. When the *Asterionella* microscope ESD was recalculated based on area of the cells, $ESD_A$, the microscope $ESD_A$ calculation produced a result more similar to the FlowCAM ABD measurement (Fig. 6).

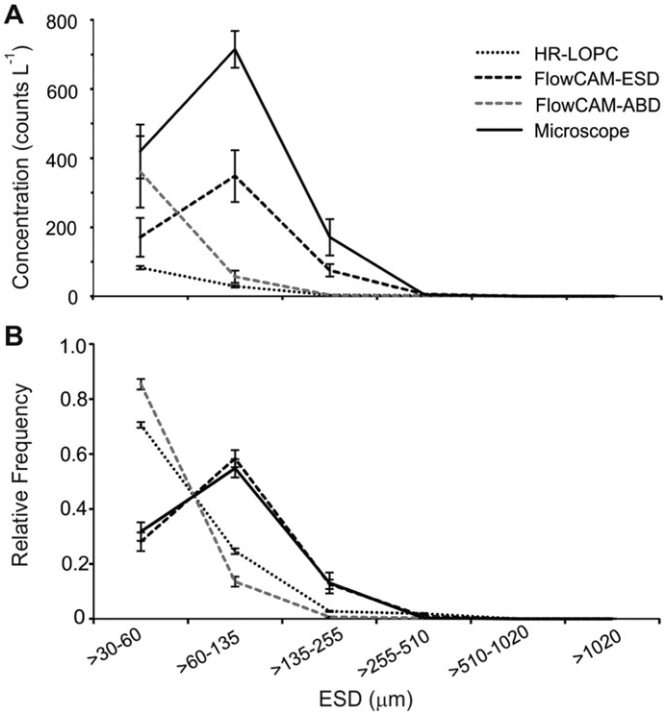


**Fig. 3.** Concentration (A) and relative frequency (B) plots for particles > 30 μm measured by the HR-LOPC, FlowCAM (organism only) ESD and ABD measurements, and the microscope.

Removal of *Asterionella* from analyses still resulted in a significant difference in the numerical concentration estimates among the FlowCAM ESD, FlowCAM ABD, HR-LOPC and microscope (one-way ANOVA, $F = 21.14$, $df = 3, 14$, $p < 0.001$) (Fig. 7A). The paired comparison showed differences between all the methods, although it is only marginal between the FlowCAM ABD and HR-LOPC ($p = 0.01$) (Table 3). Concentration estimates between methods remained significantly different when the variation among size classes were taken into account, although comparisons based on relative frequencies indicate that the distribution of particles, with removal of Asterionella, was not different across all methods except between the FlowCAM ABD and FlowCAM ESD ($p < 0.001$) (Fig. 7B and Table 2).

## 4. Discussion

The automated tools tended to underestimate particle concentration compared to standard microscopy. Manual counts of organisms on the microscope generated concentration estimates 35–60% greater than those by FlowCAM and more than two orders of magnitude greater than those by HR-LOPC. Conversion of concentration estimates to relative size frequency distributions initially resulted in nearly identical outputs from the FlowCAM ESD and microscope. The size frequency distributions generated by FlowCAM ABD and HR-LOPC remained quite different from that of the microscope, revealing important differences across methods in the measurement of particle size. For most taxa, particle size measurements generated by FlowCAM ABD were

**Table 1**
Concentration (count $L^{-1}$) of >30 μm particles, as counted by the HR-LOPC, FlowCAM and Microscope. HR-LOPC data includes all particles, while microscope data includes organisms only; FlowCAM data is presented as both total and organism-only counts.

| | HR-LOPC | FlowCAM ESD | | FlowCAM ABD | | Microscope |
|---|---|---|---|---|---|---|
| | Total | Total | Organisms | Total | Organisms | Total |
| Average | 92.0 | 861.1 | 568.0 | 552.9 | 420.9 | 1348.4 |
| Standard deviation | 7.3 | 195.6 | 119.3 | 146.8 | 102.4 | 171.1 |

**Table 2**
Results of statistical analyses comparing concentration and relative frequency estimates for > 30 μm measured by the HR-LOPC, FlowCAM (organism-only) ESD and ABD, and the microscope.

| Concentration comparison without size classes using Pair-wise comparison of methods of one-way *ANOVA* | | | |
|---|---|---|---|
| | **FlowCAM ESD** | **FlowCAM ABD** | **HR-LOPC** |
| Microscope | $F = 53.00$, $df = 1,7$, $p < 0.001$ | $F = 90.33$, $df = 1,8$, $p < 0.001$ | $F = 356.20$, $df = 1,8$, $p < 0.001$ |
| FlowCAM ESD | | *t-paired $= 9.23$, $df = 3$, $p = 0.003$ | $F = 55.26$, $df = 1,7$, $p < 0.001$ |
| FlowCAM-ABD | | | $F = 34.06$, $df = 1,7$, $p < 0.001$ |
| **Concentration comparisons with size classes using Hotelling T-squared for two multivariate independent samples** | | | |
| | **FlowCAM ESD** | **FlowCAM ABD** | **HR-LOPC** |
| Microscope | $F = 22.62$, $df = 3,5$, $p = 0.002$ | $F = 372.82$, $df = 3,5$, $p < 0.001$ | $F = 734.01$, $df = 3,6$, $p < 0.001$ |
| FlowCAM ESD | | $F = 32.75$, $df = 3,4$, $p = 0.003$ | $F = 52.43$, $df = 3,5$, $p < 0.001$ |
| FlowCAM ABD | | | $F = 24.63$, $df = 3,5$, $p = 0.002$ |
| **Relative frequency comparisons using two-sample Kolmogorov-Smirnov test with MCMC method** | | | |
| | **FlowCAM ESD** | **FlowCAM ABD** | **HR-LOPC** |
| Microscope | $p = 0.54$ | $p < 0.001$ | $p < 0.001$ |
| Flow ESD | | $p < 0.001$ | $p < 0.001$ |
| FlowCAM ABD | | | $p = 0.53$ |

*Paired-sample *t*-test was used.

more similar to microscope measurements than were those by FlowCAM ESD, though there was a mismatch in size estimates for some organisms between the FlowCAM ABD and microscope due to orientation and complex morphology. When a single problematic taxon is very abundant, the resulting size frequency distribution curves can become skewed, as was observed with *Asterionella*, though this may be resolved for well-studied aquatic ecosystems using correction factors.

It is not clear why the densities of particles measured were significantly different across methods. In contrast to our findings, previous studies have found that the standard LOPC overestimates zooplankton densities in areas with dense phytoplankton, detritus, and high turbidity (Schultes and Lopes, 2009; da Rocha Marcolin et al., 2013; Schultes et al., 2013; Checkley et al., 2008), though it has given good estimates of zooplankton abundance (Finlay et al., 2007a; Rahkola-Sorsa et al., 2014; Basedow et al., 2013). As our samples contained numerous very small and transparent particles, the HR-LOPC may have been operating at its lower sensitivity limits during our comparisons. While our findings for the FlowCAM agree with one previous study indicating underestimation of concentration compared to the microscope with preserved natural samples (Jakobsen and Carstensen, 2011), in other cases, the FlowCAM has generated higher (Álvarez et al., 2014), similar (Ide et al., 2008; Zarauz et al., 2009; Le Bourg et al., 2015) or mixed results (See et al., 2005; Garmendia et al., 2013). Discrepancies in previous studies have been attributed to comparing live cell counts to Lugol's preserved samples where cell shrinkage or breakage has occurred (Álvarez et al., 2014; Garmendia et al., 2013; Zarauz and Irigoien, 2008), but preservation should not have an effect here as all samples were similarly treated. Lower concentration estimates on our instruments could be due to particles being missed or error in the measurement of analysis volume by the instruments.

In terms of measurement accuracy, the FlowCAM ABD generated particle size estimates equivalent to the microscope calculated ESD for most individual taxonomic groups, whereas the FlowCAM ESD measurements were larger. Similar results have been reported in other studies (Jakobsen & Carstensen, 2011; Álvarez et al., 2014). Our study found large differences in size estimates of taxa that could be considered morphologically complex (*Asterionella*, *Closteriopsis*, *Staurastrum*, and Bosminids). Previous researchers have also found size differences between the FlowCAM and other instruments when measuring asymmetrical and chain-forming diatoms due to orientation in the flow cell (Jakobsen and Carstensen, 2011; Spaulding et al., 2012). Particle orientation is similarly flexible for the LOPC, resulting in smaller size estimates than taken by microscopy, especially for laterally flattened organisms like cladocerans, when the narrow depth versus the wider width is measured by the occultation of the laser (Finlay et al., 2007a; Rahkola-Sorsa et al., 2014). Organisms measured on the microscope

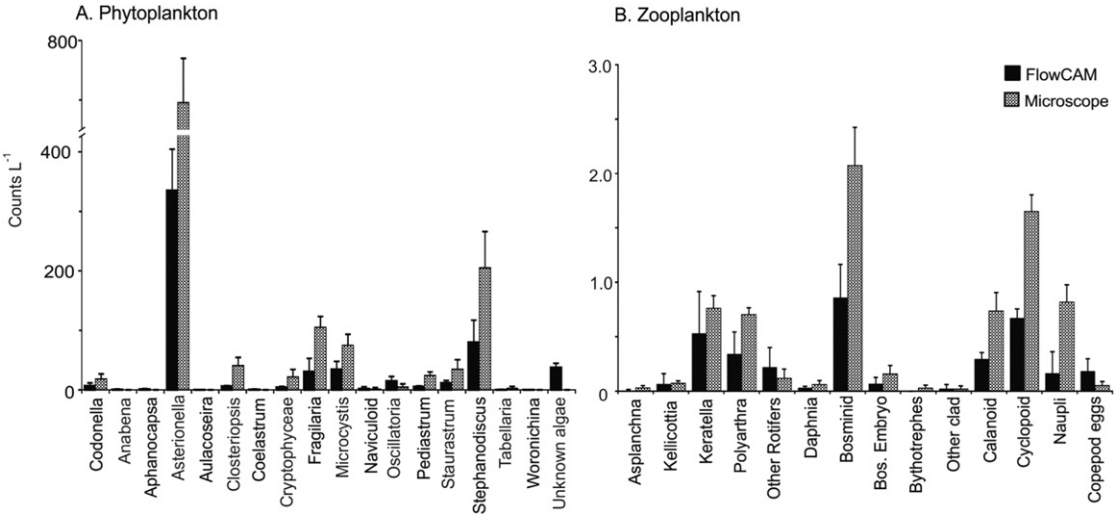


**Fig. 4.** Concentration estimates for A) phytoplankton and B) zooplankton taxonomic groups counted on the FlowCAM and microscope. Error bars indicate standard deviation of the mean.

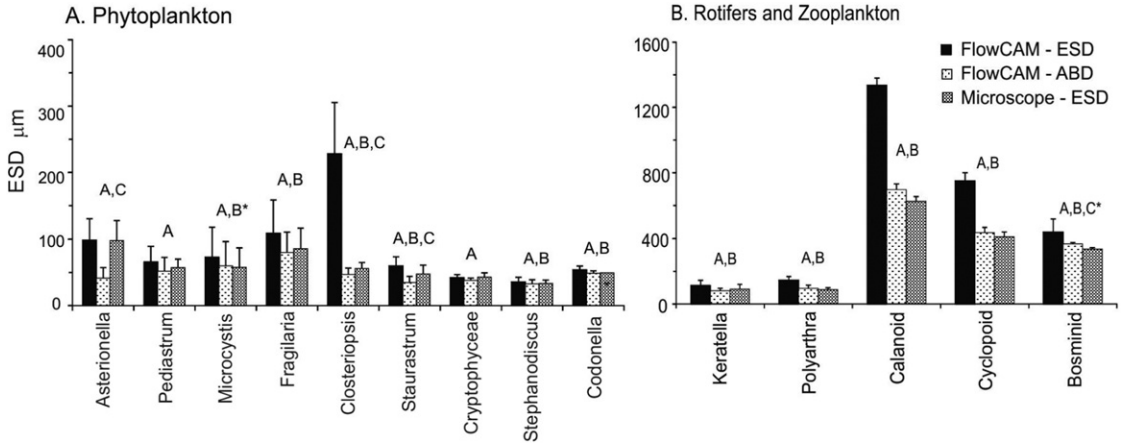


**Fig. 5.** Average size (+ standard deviation) of A) phytoplankton and B) zooplankton taxonomic groups measured on the microscope and FlowCAM (both ESD and ABD). Significant differences (ANOVA with Bonferroni, $p < 0.0001$) between FlowCAM ESD and FlowCAM ABD indicated by 'A', between FlowCAM ESD and the microscope by 'B' and between FlowCAM ABD and the microscope by 'C', * indicates marginally significant.

tend to lay flat allowing length and width to be measured accurately, but with both FlowCAM and LOPC, particles can pass the camera/laser along any axis such that length and width measurements can be taken along any orientation of the particle. While this variability in orientation tends to skew results towards underestimation in comparison with traditional microscopy, the automated tools may be better able to measure the true minimum dimension of an organism, as written in Regulation D-2, when depth is the narrowest axis.

In this study, differences in the size measurements between the FlowCAM ABD and the microscope ESD for the star-shaped colony *Asterionella*, combined with high colony abundance in the sample, influenced the shape of the size frequency distribution curves. The FlowCAM ABD size frequency distribution peaked at 45 µm with *Asterionella*, whereas the peak occurred at 90 µm for the microscope ESD particle curve. The microscope calculated ESD used the length and width of the whole colony and agreed well with the similarly measured FlowCAM ESD using feret lines, whereas the FlowCAM ABD was based on the area of the cells. Changing the size estimate on the microscope to be based on the area of the cells excluding the interstitial space corrected the difference between the microscope ESD and FlowCAM ABD giving a more similar size estimate. Normally, when measuring phytoplankton on the microscope, cells within the colony are measured individually; thus, special consideration is needed when utilizing automated tools to analyse samples containing colonies. Re-analysis of the size frequency distributions with the removal of *Asterionella* from FlowCAM and microscope data resulted in more similar curves across methods with FlowCAM ABD having the best fit compared to the microscope, although microscope concentration estimates were still significantly higher than estimates by the other methods.

With the removal of *Asterionella*, the FlowCAM ABD and the HR-LOPC particle size frequency distribution curves were very similar in both shape and concentration, though the HR-LOPC was still measuring relatively low at the bottom end of the size spectrum (<60 µm) compared to the FlowCAM. Rolinski et al. (2013) found similar issues with size measurements of *Asterionella* on another particle counter. It is possible that the HR-LOPC is underestimating phytoplankton densities due to orientation or transparency. The LOPC measures particles by determining the occultation of a laser beam captured by, in this case, 30 × 30 µm diode elements (Herman et al., 2004, Rolls Royce Rolls Royce Canada Ltd. – Naval Marine). Laterally flattened colonial phytoplankton like *Fragilaria* and *Asterionella* or filamentous algae may not be captured by the HR-LOPC if the narrow axis (depth) is oriented

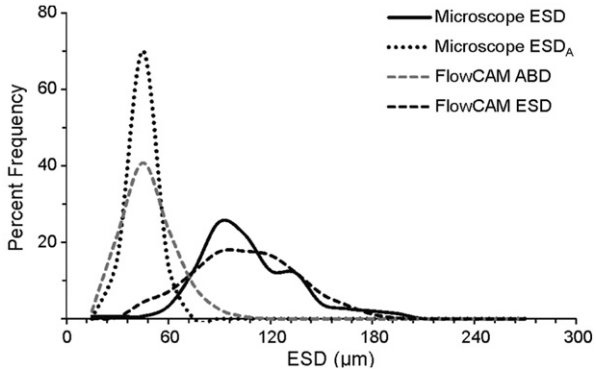


**Fig. 6.** Comparison of different ESD calculations used to measure *Asterionella* by microscope and FlowCAM. Microscope ESD is based on the colony length and width and Microscope ESD$_A$ is based on the area of the individual cells in the colony.

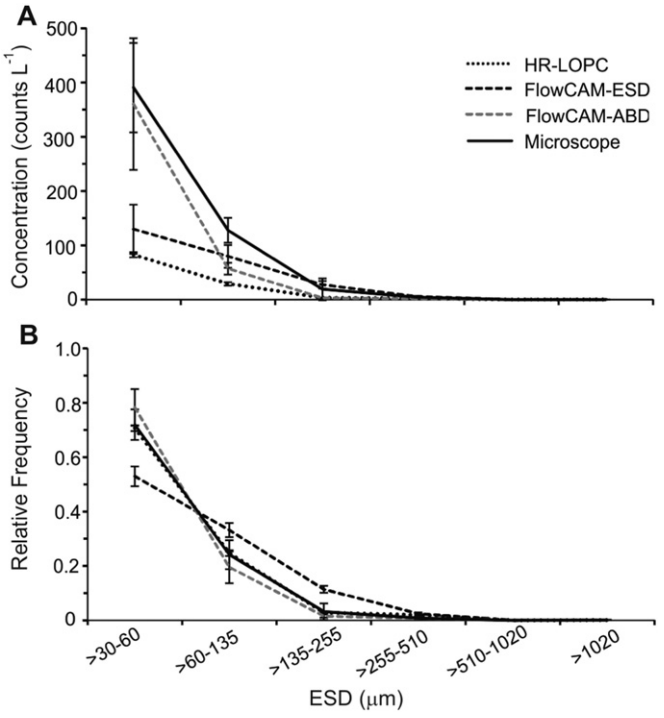


**Fig. 7.** Particle size distributions without *Asterionella* measured by the microscope, FlowCAM ESD and FlowCAM ABD plotted with total particle counts on the HR-LOPC for both A) frequency in counts $L^{-1}$ and B) relative frequency with standard deviations.

**Table 3**
Statistical analysis results for comparing the size frequency distribution between HR-LOPC, FlowCAM (organism only) ESD and ABD measurements, and the microscope with *Asterionella* removed from the FlowCAM and microscope data.

| Concentration comparison without size classes using Pair-wise comparison of methods of one-way *ANOVA* | | | |
|---|---|---|---|
| | **FlowCAM ESD** | **FlowCAM ABD** | **HR-LOPC** |
| Microscope | $F = 25.51$, df = 1,7, $p = 0.002$ | $F = 15.63$, df = 1,7, $p = 0.006$ | $F = 87.86$, df = 1,8, $p < 0.001$ |
| FlowCAM ESD | | *t-paired = 0.01, df = 3, $p = 0.99$ | $F = 14.42$, df = 1,7, $p = 0.007$ |
| FlowCAM ABD | | | $F = 4.49$, df = 1,7, $p = 0.07$ |
| **Concentration comparisons with size classes using Hotelling T-squared for two multivariate independent samples** | | | |
| | **FlowCAM ESD** | **FlowCAM ABD** | **HR-LOPC** |
| Microscope | $F = 65.24$, df = 3,5, $p < 0.001$ | $F = 17.67$, df = 3,5, $p = 0.004$ | $F = 304.76$, df = 3,6, $p < 0.001$ |
| FlowCAM ESD | | $F = 16.88$, df = 3,4, $p = 0.010$ | $F = 20.78$, df = 3,5, $p = 0.003$ |
| FlowCAM ABD | | | $F = 24.61$, df = 3,5, $p = 0.002$ |
| **Relative frequency comparisons using two-sample Kolmogorov-Smirnov test with MCMC method** | | | |
| | **FlowCAM ESD** | **FlowCAM ABD** | **HR-LOPC** |
| Microscope | $p = 0.10$ | $p = 0.75$ | $p = 1.00$ |
| FlowCAM ESD | | $p < 0.001$ | $p = 0.48$ |
| FlowCAM ABD | | | $p = 0.77$ |

*Paired-sample *t*-test was used.

towards the laser and is below the detection threshold. In addition, our samples were preserved in ethanol reducing the opacity of the phytoplankton particles, which may reduce the ability of the particle to occult (block) the laser beam. Further investigation would be needed at the lower size limit (30–105 μm, nominally phytoplankton, rotifers and naupli) of the HR-LOPC to resolve if, and how effectively, it is capturing the smaller particles and to determine if capture rate improves when working with an unpreserved sample.

The results of our study indicate that both automated tools can generate frequency distributions of particles that might be particularly useful if correction factors can be developed for known differences in well-studied aquatic ecosystems. In terms of 'rapid' compliance monitoring for organisms ≥50 μm in ballast water, only the HR-LOPC can analyse an entire sample in a rapid timeframe (minutes) whereas only small subsample volumes can be run on the FlowCAM in short order. In this study the processing time (running the sample and sorting the images) on the FlowCAM was equivalent to the microscope work with the inclusion of measuring particles (though this is typically not conducted for ballast water evaluations). Future work using the FlowCAM to assess ≥50 um particles could eliminate the use of the 80 μm flow cell, as the resolution of the 300 μm flow cell is 30 μm, in order to decrease the processing time by one third, if not more. The concentration of dead particles and debris will increase the time or decrease the volume of sample that can be processed by the FlowCAM and microscope, but it is not clear if both methods would be impacted equally.

Future work is needed to assess the transferability of our findings to samples from a diverse array of aquatic ecosystems and to determine if these automated tools can be used to assess viability of particles in a sample. The FlowCAM is able to measure both fluorescence and colour and can detect vital stains (Peterson and Nelson 2010; Veldhuis and Fuhr, 2008), though this was not tested here. It may also be important to quantify any error associated with the assessment of live organisms, as live individuals may be able to swim against the current within the automated devices, possibly resulting in duplicate counting. Another issue to explore when validating these tools for compliance monitoring is the enumeration of colonies as one entity even though it is composed of a number of smaller cells. Reavie and fellow researchers (2010) deemed the FlowCAM unsuitable for enumerating particles 10–50 μm due to the presence of colonial cells, indicating that examining images of individuals in colonies to generate accurate counts would take a significant amount of time. For the ≥50 μm organisms, colonies consisting mainly of cells <50 μm can be filtered out by the FlowCAM software - automated classification by the FlowCAM has been shown to have an overall error around 10% (Álvarez et al., 2014 and citations therein). Imaging of particles, especially those deemed viable, would be an advantageous feature for an indicative analysis tool by providing a permanent data record; it would also allow trained users to verify or correct data outputs or to identify problematic samples, such as samples dominated by colonial phytoplankton species.

## Acknowledgements

Financial support was provided by Transport Canada, and Fisheries and Oceans Canada. EB acknowledges support from the Alexander von Humboldt Sofja Kovalevskaja Award. This paper presents the results of systematic investigative research, and neither endorses nor discourages the use of the technologies tested.

## References

(IMO) International Maritime Organization, 2004. International Convention For The Control And Management Of Ships' Ballast Water And Sediments (Adopted 13 February 2004).

Álvarez, E., López-Urrutia, Á., Nogueira, E., Fraga, S., 2011. How to effectively sample the plankton size spectrum? A case study using FlowCAM. J. Plankton Res. 33 (7): 1119–1133. http://dx.doi.org/10.1093/plankt/fbr012.

Álvarez, E., López-Urrutia, Á., Nogueira, E., 2012. Improvement of plankton biovolume estimates derived from image-based automatic sampling devices: application to FlowCAM. J. Plankton Res. 34 (6):454–469. http://dx.doi.org/10.1093/plankt/fbs017.

Álvarez, E., Moyano, M., López-Urrutia, Á., Nogueira, E., Scharek, R., 2014. Routine determination of plankton community composition and size structure: a comparison between FlowCAM and light microscopy. J. Plankton Res. 36 (1):170–184. http://dx.doi.org/10.1093/plankt/fbt069.

Bailey, S.A., 2015. An overview of thirty years of research on ballast water as a vector for aquatic invasive species to freshwater and marine environments. Aquat. Ecosyst. Health Manag. 18 (3), 261–268.

Basedow, S.L., Tande, K.S., Norrbin, M.F., Kristiansen, S.A., 2013. Capturing quantitative zooplankton information in the sea: performance test of laser optical plankton counter and video plankton recorder in a *Calanus finmarchicus* dominated summer situation. Prog. Oceanogr. 108:72–80. http://dx.doi.org/10.1016/j.pocean.2012.10.005.

Beaulieu, S.E., Mullin, M.M., Tang, V.T., Pyne, S.M., King, A.L., Twining, B.S., 1999. Using an optical plankton counter to determine the size of distributions of preserved zooplankton samples. J. Plankton Res. 21:1939–1956. http://dx.doi.org/10.1093/plankt/21.10.1939.

Bradie, J., 2016. Report on Performance of Ballast Water Collection and Analysis Devices. Reference 0800Z11-1111/001 ReBat, Federal Maritime and Hydrographic Agency, Hamburg, Germany (130 pp. Available at: http://www.bsh.de/de/Meeresdaten/Umweltschutz/ReBaT-Projekt/index.jsp).

Carlton, J.T., 1985. Trans-oceanic and interoceanic dispersal of coastal marine organisms: the biology of ballast water. Oceanogr. Mar. Biol. Annu. Rev. 23, 313–371.

Carlton, J.T., Geller, J.B., 1993. Ecological roulette: the global transport of nonindigenous marine organisms. Science 261, 78–82.

Checkley Jr, D.M., Davis, R.E., Herman, A.W., Jackson, G.A., Beanlands, B., Regier, L.A., 2008. Assessing plankton and other particles in situ with the SOLOPC. Limnol. Oceanogr. 53 (5):2123–2136. http://dx.doi.org/10.4319/lo.2008.53.5_part_2.2123.

da Rocha Marcolin, C., Schultes, S., Jackson, G.A., Lopes, R.M., 2013. Plankton and seston size spectra estimated by the LOPC and ZooScan in the Abrolhos Bank ecosystem (SE Atlantic). Cont. Shelf Res. 70:74–87. http://dx.doi.org/10.1016/j.csr.2013.09.022.

Finlay, K., Beisner, B.E., Barnett, A.J.D., 2007a. The use of the Laser Optical Plankton Counter to measure zooplankton size, abundance, and biomass in small freshwater lakes. Limnol. Oceanogr. Methods 5:41–49. http://dx.doi.org/10.4319/lom.2007.5.41/pdf.

Finlay, K., Beisner, B.E., Patoine, A., Pinel-Alloul, B., 2007b. Regional ecosystem variability drives the relative importance of bottom-up and top-down factors for zooplankton size spectra. Can. J. Fish. Aquat. Sci. 64 (3):516–529. http://dx.doi.org/10.1139/f07-028.

First, M.R., Drake, L.A., 2012. Performance of the human "counting machine": evaluation of manual microscopy for enumerating plankton. J. Plankton Res. 34 (12): 1028–1041. http://dx.doi.org/10.1093/plankt/fbs068.

Gaardsted, F., Tande, K.S., Basedow, S.L., 2010. Measuring copepod abundance in deep-water winter habitats in the NE Norwegian Sea: intercomparison of results from laser optical plankton counter and multinet. Fish. Oceanogr. 19:480–492. http://dx.doi.org/10.1111/j.1365-2419.2010.00558.

Gaardsted, F., Tande, K.S., Pedersen, O.P., 2011. Vertical distribution of overwintering *Calanus finmarchicus* in the NE Norwegian Sea in relation to hydrography. J. Plankton Res. 33 (10):1477–1486. http://dx.doi.org/10.1093/plankt/fbr042.

Garmendia, M., Revilla, M., Zarauz, L., 2013. Testing the usefulness of a simple automatic method for particles abundance and size determination to derive cost-effective biological indicators in large monitoring networks. Hydrobiologia 704 (1):231–252. http://dx.doi.org/10.1007/s10750-012-1400-x.

Herman, A.W., Beanlands, B., Phillips, E.F., 2004. The next generation of optical plankton counter: the laser-OPC. J. Plankton Res. 26 (10):1135–1145. http://dx.doi.org/10.1093/plankt/fbh095.

Ide, K., Takahashi, K., Kuwata, A., Nakamachi, M., Saito, H., 2008. A rapid analysis of copepod feeding using FlowCAM. J. Plankton Res. 30 (3):275–281. http://dx.doi.org/10.1093/plankt/fbm108.

Jakobsen, H.H., Carstensen, J., 2011. FlowCAM: sizing cells and understanding the impact of size distributions on biovolume of -planktonic community structure. Aquat. Microb. Ecol. 65 (1):75–87. http://dx.doi.org/10.3354/ame01539.

Jørgensen, C., Gustavson, K., Hansen, J.B., Hies, T., 2010. Development of guidance on how to analyze a ballast water sample. DHI, Final Report to: The European Maritime Safety Agency (EMSA) (December 2010).

Le Bourg, B., Cornet-Barthaux, V., Pagano, M., Blanchot, J., 2015. FlowCAM as a tool for studying small (80–1000 μm) metazooplankton communities. J. Plankton Res. 37 (4):666–670. http://dx.doi.org/10.1093/plankt/fbv025.

Mines, C.H., Ghadouani, A., Legendre, P., Yan, N.D., Ivey, G.N., 2013. Examining shifts in zooplankton community variability following biological invasion. Limnol. Oceanogr. 58 (1):399–408. http://dx.doi.org/10.4319/lo.2013.58.1.0399.

Peterson, K., Nelson, H., 2010. New data experiments using viability stains on treated ballast water for IMO compliance monitoring pp. 241–245. In: Bellefontaine, N., Haag, H., Lidén, O., Matheickal, J. (Eds.), Emerging Ballast Water Management Systems. Proceedings of the IMO-WMU research and Development Forum 26–29, Malmö, Sweden. Available online at: http://globallast.imo.org/wp-content/uploads/2015/01/EmergingBallastWater.pdf.

Rahkola-Sorsa, M., Voutilainen, A., Viljanen, M., 2014. Intercalibration of an acoustic technique, two optical ones, and a simple seston dry mass method for freshwater zooplankton sampling. Limnol. Oceanogr. Methods 12:102–113. http://dx.doi.org/10.4319/lom.2014.12.102.

Reavie, E.D., Cangelosi, A.A., Allinger, L.E., 2010. Assessing ballast water treatments: evaluation of viability methods for ambient freshwater microplankton assemblages. J. Great Lakes Res. 36 (3):540–547. http://dx.doi.org/10.1016/j.jglr.2010.05.007.

Rolinski, S., Pätz, P., Papendick, K., Jähnichen, S., Scheifhacken, N., 2013. Phytoplankton appearance in particle size spectra - deriving conversion functions between microscopic and particle counter measurements. Water Res. 47 (5):1928–1940. http://dx.doi.org/10.1016/j.watres.2013.01.024.

Ruiz, G.M., Fofonoff, P.W., Carlton, J.T., Wonham, M.J., Hines, A.H., 2000. Invasion of coastal marine communities in North America: apparent patterns, processes, and biases. Annu. Rev. Ecol. Syst. 31, 481–531.

See, J.H., Campbell, L., Richardson, T.L., Pinckney, J.L., Shen, R., Guinasso, N.L., 2005. Combining new technologies for determination of phytoplankton community structure in the Northern Gulf of Mexico 1. J. Psychol. 41 (2):305–310. http://dx.doi.org/10.111/j.1529-8817.2005.04132.x.

Schultes, S., Lopes, R.M., 2009. Laser optical plankton counter and zooscan intercomparison in tropical and subtropical marine ecosystems. Limnol. Oceanogr. Methods 7: 771–784. http://dx.doi.org/10.4319/lom.2009.7.771.

Schultes, S., Sourisseau, M., Le Masson, E., Lunven, M., Marié, L., 2013. Influence of physical forcing on mesozooplankton communities at the Ushant tidal front. J. Mar. Syst. 109: S191–S202. http://dx.doi.org/10.1016/j.jmarsys.2011.11.025.

Sieracki, C.K., Sieracki, M.E., Yentsch, C.S., 1998. An imaging-in-flow system for automated analysis of marine microplankton. Mar. Ecol. Prog. Ser. 168:285–296. http://dx.doi.org/10.3354/meps168285.

Spaulding, S.A., Jewson, D.H., Bixby, R.J., Nelson, H., McKnight, D.M., 2012. Automated measurement of diatom size. Limnol. Oceanogr. Methods 10:882–890. http://dx.doi.org/10.4319/lom.2012.10.882.

Steinberg, M.K., First, M.R., Lemieux, E.J., Drake, L.A., Nelson, B.N., Kulis, D.M., Anderson, D.M., Welschmeyer, N.A., Herring, P.R., 2012. Comparison of techniques used to count single-celled viable phytoplankton. J. Appl. Phycol. 24 (4):751–758. http://dx.doi.org/10.1007/s10811-011-9694-z.

Veldhuis, M.J.W., Fuhr, F., 2008. Final Report of the Land-Based and Shipboard Testing of the SEDNA®-System. NIOZ Royal Netherlands Institute for Sea Research. Texel, Netherlands.

Zarauz, L., Irigoien, X., 2008. Effects of Lugol's fixation on the size structure of natural nano–microplankton samples, analyzed by means of an automatic counting method. J. Plankton Res. 30 (11):1297–1303. http://dx.doi.org/10.1093/plankt/fbn084.

Zarauz, L., Irigoien, X., Fernandes, J.A., 2009. Changes in plankton size structure and composition, during the generation of a phytoplankton bloom, in the central Cantabrian sea. J. Plankton Res. 31 (2), 193–207.

Zetsche, E.M., Meysman, F.J., 2012. Dead or alive? Viability assessment of micro-and mesoplankton. J. Plankton Res. 34 (6):493–509. http://dx.doi.org/10.1093/plankt/fbs018.